$BaLa_5V_2O_3N_7$: A Novel Anti-Perovskite Oxynitride for Electrode Applications

Shi-Rui Zhang, [a] Xiao-Ming Wang,*[a] Lei-Ming Fang, [b] Jia-Chen Li, [a] Ying-Ying Xu,[a] Zi-Han Ren,[a] Zu-Pei Yang, [c] Xiao-Jun Kuang,*[d] and Huan Jiao*[a]

Electronic Supplementary Information (ESI):

Materials and synthesis.

Synthesis of $BaLa_5V_2O_3N_7$ single crystal

A single crystal $BaLa_5V_2O_3N_7$ was prepared by ammonothermal method with the addition of Li_3N/LiF as the flux. 0.7 g of Ba_3N_2 (99.5%, Hebei LiFu), 0.5 g of LaN (99%, Xierde), 0.1 g of V_2O_5 (99%, aladdin), 0.1 g of Li_3N (99%, Hebei LEDphor Optoelectronics Technology Co.,LTD.), and 0.2 g of LiF (99%, aladdin) reaction materials were successively weighed and ground evenly in an agate mortar. The homogeneous powders were then transferred to a tungsten crucible with a lid and sealed with a sealing film. All the above steps were carried out in an Argon-filled glovebox (H_2O < 0.1 ppm, O_2 < 0.1 ppm). Subsequently, transfer the crucible to the high-pressure reactor, flush into about 0.6 MPa ammonia gas, seal the reactor. Next, Set the heating program, the temperature rises to 1080°C at a rate of 3°C/min, constant temperature for 10 h to promote the full reaction of raw materials. Then the temperature was slowly cooled to 600°C at a rate of 0.32°C/min to promote the growth of crystal nuclei. Finally, the samples were naturally cooled to room temperature to obtain black tetragonal bulk crystals.

Synthesis of $BaLa_5V_2O_3N_7$ polycrystalline samples

Two polycrystalline powder samples $BaLa_5V_2O_3N_7$ were successfully prepared by traditional high temperature solid phase method, in N_2 (90%)/H_2 (10%) atmosphere. Binary nitride was selected as the starting material (oxygen in the product was provided by the oxygen components remaining in the reducing atmosphere). The raw materials Ba_3N_2, LaN and VN were weighed into the agate mortar, fully grind for 30 min, and transferred to the tungsten crucible for sealing. All the above steps were carried out in an Argon-filled glovebox (H_2O < 0.1 ppm, O_2 < 0.1 ppm). Finally, a tungsten crucible was placed in a tubular furnace for calcination at 1400°C for 10 h, and the pure phase powders were collected for characterization.

Characterizations

Single Crystal X-ray Diffraction. The Single-crystal X-ray diffraction (XRD) data was collected on Rigaku diffraction (XtaLAB Synergy-R) with a microfocus rotating anode X-ray source diffractometer. The crystal structure of $BaLa_5V_2O_3N_7$ was solved by SHELXT and refined by SHELXL utilizing Olex2 as a graphical interface. Further details on the crystalstructure investigation can be obtained from the Cambridge Crystallographic Data Centre (CCDC) on quoting the depository number CCDC code 2259152.

Powder X-ray Diffraction. X-ray diffraction (XRD) data were collected using a Rigaku MiniFlex600 (Japan) diffractometer (Cu Kα radiation, D/teX Ultra high-speed 1D detector). Data collections were carried out over a 2θ range from 5° to 120° in a step-mode with 0.02°. Rietveld refinement for $BaLa_5V_2O_3N_7$ was performed with TOPAS5 software.

Neutron powder diffraction (NPD). NPD at the neutron beamline of the China Mianyang Research Reactor. For the NPD experiments, the incident neutron wavelengths for $BaLa_5V_2O_3N_7$ was λ = 1.5915 Å. Structure analysis was performed using the Rietveld method with the TOPAS 5 software.

Variable-temperature X-ray diffraction (VT-XRD). VT-XRD was collected from room temperature to 200°C and 200°C to 400°C at intervals of 50°C and 20°C in the range of 10–80°, allowing 5 min for temperature equilibration before collecting the data sets for 30 min at each set point.

SEM + EDX. The morphology of the crystalline sample for $BaLa_5V_2O_3N_7$ powder was investigated by scanning electron microscopy (SEM, Philips-FEI Quanta 25, America) at an accelerating voltage of 5 kV. The chemical composition was confirmed by an attached energy dispersive X-ray spectrometer (Bruker EDX-XFlash6/30 detector) at an accelerating voltage of 12.5 kV.

UV/vis Spectroscopy. The diffuse reflection spectrum was measured on a Lambd 1050 UV-vis-NIR spectrophotometer (Perkin-Elmer) in the range from 200 nm to 1350 nm with 1 nm per step size, while the white powder $BaSO_4$ was used as a reference standard.

Differential Scanning Calorimetry (DSC). The DSC profiles were recorded in a simultaneous thermal analysis system (America, Q-600/Q1000). An approximately 10 mg finely ground sample was packed in an alumina cup, and the temperature was raised from 30 to 800°C at a rate of 5°C /min in air.

TEM and HRTEM. Transmission electron microscopy and high-resolution TEM characterizations were carried out using a field emission transmission electron microscope at 200 kV (America, Tecnai G2 F20).

X-ray photoelectron spectroscopy (XPS). X-ray photoelectron spectroscopy analyses were conducted on an Axis UltraDLD (Britain) X-ray photoelectron spectrometer operating.

Electron paramagnetic resonance (EPR). Continuous-wave X-band EPR spectra were recorded on a Bruker E500 spectrometer with a dual-mode microwave cavity.

Density Functional Theory (DFT). The band structure and density of states (DOS) of $BaLa_5V_2O_3N_7$ calculations were performed using density functional theory (DFT) and the Cambridge Serial Total Energy Package (CASTEP) code. The plane-wave basis set was chosen for the expansion of valence-electron wave functions at the local density approximation (LDA) level. The crystal structure was optimized by using the Broyden-Fletcher-Goldfarb-Shannon (BFGS) method. The band structure and density of states (DOS) were calculated where eigenenergy convergence of self-consistent field (SCF) was within 1.0×10^{-7} eV/atom. 340 eV was selected as energy cutoff of plane wave basis, and 2×2×1 Monkhorst-Pack grid (separation ~0.04 $Å^{-1}$) was chosen as K-point sampling in the process of calculations. Furthermore, the co-occupied Ba/La and O/N sites were separated by reducing the space group symmetry to P1 (No.1). According to the ratio of co-occupied ions, each site was identified with a specific atom to avoid CASTEP calculation errors.

Electrochemical measurements. Alternating-current (AC) impedance spectroscopy measurements were carried out in a conventional four- probe direct current method at an electrochemical station (CHI 660E), response analyzer over a frequency range of 10^{-1}-10^{6} Hz within the 25-400°C temperature range in High purity Ar_2 gas flowing (99.999%) at 50 mL min^{-1}. Prior to impedance spectroscopy measurements, a quick-drying conductive silver paste was coated on the upper and lower surfaces of the ceramic sheet and heat treated at 50°C for 30 minutes to promote the decomposition of organic components in the paste and the formation of electrodes. Prior to the impedance measurement, the temperature was equilibrated at each set point for 15 min. The ZView software was used to analyze the impedance data. The activation energies, E_a, for the conductivities were estimated using the Arrhenius equation:[1]

$$\sigma = \frac{A_0}{T} exp\left(-\frac{E_a}{kT}\right)$$

where A_0, k, and T correspond to the pre-exponential factor, Boltzmann constant, and absolute temperature, respectively.

Evaluation of Polarization Resistance and Fuel Cell Performance. DC functionality of the system was utilized to attain the characteristic *V–I* and *P–I* curves using an electrochemical station (VSP, Bio-Logic, France).[1] The curves of the $BaLa_5V_2O_3N_7|Bi_4Ba_{0.17}V_{1.83}O_{10.745-\sigma}|Sr_{0.3}La_{0.7}MnO_3$ and $Pt|Bi_4Ba_{0.17}V_{1.83}O_{10.745-\sigma}|Sr_{0.3}La_{0.7}MnO_3$ cells were recorded at different temperatures, ranging from 200 to 300°C. For fuel cell electrochemical performance characterization, the effective surface area of this cell was kept to 0.8 cm^2. A flow of 300 mL min^{-1} dry N_2/H_2 (95%/5%) was employed as fuel on the anode side, while O_2 was fed into the cathode at the same flow.

Table of Contents

Table S1. Selected interatomic distances and angles for $BaLa_5V_2O_3N_7$.

bond length	(Å)		
La1-O2	2.550(4)		
La1-N/O1	2.470(8)		
La1-N/O1	2.771(7)		
Ba/La2-O2	2.835(6)		
Ba/La2-N/O1	2.873(7)		
V-N/O1	1.806(7)		
bond angle	(deg)		
N/O1-V-N/O1	113.1(5)	102.5(5)	
O2-Ba/La2-N/O1	66.8(1)	113.1(1)	
N/O1-Ba/La2-N/O1	81.0(1)	63.3(3)	139.4(3)
N/O1-La-N/O1	90.7(3)	87.3(4)	149.4(3)
O2-La-N/O1	77.4(1)	72.2(1)	131.7(1)

Note: The Ba/La2–O/N band length is between 2.835(6) Å and 2.873(7) Å, which is not common in the reported Ba/La co-occupied nitrogen oxides, such as $Ba_{22.74}La_{54.84}(Si_{129}N_{240})O_3$: Ba/La–O 2.337(8) Å;[2] $La_3BaSi_5N_9O_2$: Ba/La–O 2.475(2)–2.499(4) Å;[3] $LaBa_2Ta_5O_{13}N_2$: Ba/La–O/N 2.669(2)–2.707(2) Å.[4] The distances V–(O,N) (see Tab. S1) within the $[VO_{0.5}N_{3.5}]^{6.5+}$ unit is 1.806(7) Å. The angles N/O1–V–N/O1 are close to the regular tetrahedral angle. The size of bond length is lower than that the typical V–(O,N) range of oxynitrides reported so far, such as Ba_2VO_3N: 1.713(2)–1.740(2) Å;[5] $NdVO_2N$: 1.959(7)–2.003(1) Å;[6] $LaVO_{2.78}N_{0.1}$: 2.000(2)–2.002(4) Å;[7] $V_3O_{4.61}N_{0.27}$: 1.880(3)–2.204(2) Å.[8]

Table S2. Atomic coordinates, equivalent displacement parameters, and site occupancies of $BaLa_5V_2O_3N_7$ at 293 K.

atom	*x*	*y*	*z*	U_{eq}	Wyck.	Occupancy
La1	0.1716(1)	0.3283(9)	0.5000(0)	0.4130(0)	8h	1.000
Ba1	0.5000(0)	0.5000(0)	0.2500(0)	0.6130(0)	4a	0.500
La2	0.5000(0)	0.5000(0)	0.2500(0)	0.6130(0)	4a	0.500
V1	0.5000(0)	0.0000(0)	0.2500(0)	0.3260(0)	4b	1.000
N1	0.3555(9)	0.1445(9)	0.3498(7)	1.2416(0)	16l	0.875
O1	0.3555(9)	0.1445(9)	0.3498(7)	1.2416(0)	16l	0.125
O2	0.5000(0)	0.5000(0)	0.5000(0)	1.6300(0)	4c	1.000

Table S3. Anisotropic Displacement Parameters ($Å^2$) for $BaLa_5V_2O_3N_7$ at 293 K.

Atom	U_{11}	U_{22}	U_{33}	U_{12}	U_{13}	U_{23}
La1	0.005 (1)	0.005(1)	0.004(1)	-0.000(4)	0.000(0)	0.000(0)
Ba1	0.007(1)	0.007(1)	0.005(0)	0.000(0)	0.000(0)	0.000(0)
La2	0.007(1)	0.007(1)	0.005(0)	0.000(0)	0.000(0)	0.000(0)
V1	0.004(1)	0.004(1)	0.003(0)	0.000(0)	0.000(0)	0.000(0)
N1	0.013(2)	0.013(2)	0.012(3)	0.004(3)	0.000(2)	0.000(2)
O1	0.013(2)	0.013(2)	0.012(3)	0.004(3)	0.000(2)	0.000(2)
O2	0.012(4)	0.012(4)	0.025(7)	0.000(0)	0.000(0)	0.000(0)

Table S4. Crystallographic data of $BaLa_5V_2O_3N_7$ derived from Rietveld refinement of X-ray and Neutron data.

	X-ray	neutron
Crystal system	Tetragonal	
Space group	*I*4/*mcm* (No. 140)	
Cell parameters /Å	*a* = 6.8623(2), *c* = 11.3805(3)	*a* = 6.8735(11), c = 11.3797(19)
Cell volume /Å^3	535.93(3)	537.64(19)
Formula units /cell	Z = 4	
Structure refinement	Topas 5	
Temperature (K)	293	
Profile function	PV_TCHZ	
Radiation	Cu Kα	neutron (λ = 1.5915 Å)
2ϑ range (º)	10-120	10-160
Step size (º)	0.02	0.1
R_{wp} / R_p	0.0609 / 0.0452	0.0214 / 0.0168
GOF	1.82	1.46

Table S5. Refine Atomic Coordinates for $BaLa_5V_2O_3N_7$ from CW-Neutron data Collected

atom	*x*	*y*	*z*	U_{eq}	*Wyck.*	occupancy
La1	0.1757(1)	0.3242(9)	0.5000(0)	0.8640(0)	8h	1.00(0)
Ba1	0.5000(0)	0.5000(0)	0.2500(0)	0.5108(0)	4a	0.50(4)
La2	0.5000(0)	0.5000(0)	0.2500(0)	0.1619(0)	4a	0.50(2)
V1	0.5000(0)	0.0000(0)	0.2500(0)	0.5021(0)	4b	1.00(0)
N1	0.3559(6)	0.1440(4)	0.3492(5)	1.1310(0)	16l	0.87(1)
O1	0.3559(6)	0.1440(4)	0.3492(5)	1.7770(0)	16l	0.13(1)
O2	0.5000(0)	0.5000(0)	0.5000(0)	1.5770(0)	4c	1.00(0)

Table S6. The fitting parameters extracted from ZView with an equivalent circuit of $(R_1CPE_1)(R_2CPE_2)$,

where R represents a resistance, and the constant phase element (CPE) representing a non-ideal capacitor. The R and CPE have the units of Ω cm^2 and F cm^{-2}, respectively.[9]

T(°C)	R_1	CPE_1-T	CPE_1-P	R_2	CPE_2-T	CPE_2-P
300	1.6937E6	3.980E-11	0.95248	1.000E+20	3.2022E-6	0.46429
350	437770	3.786E-11	0.96158	1.000E+20	7.6319E-6	0.36617

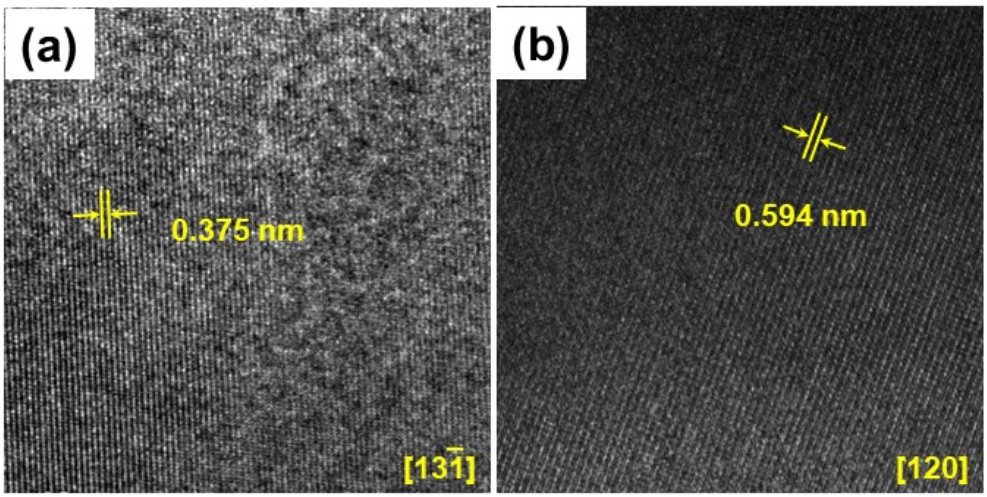

Figure S1. The HRTEM of $BaLa_5V_2O_3N_7$.

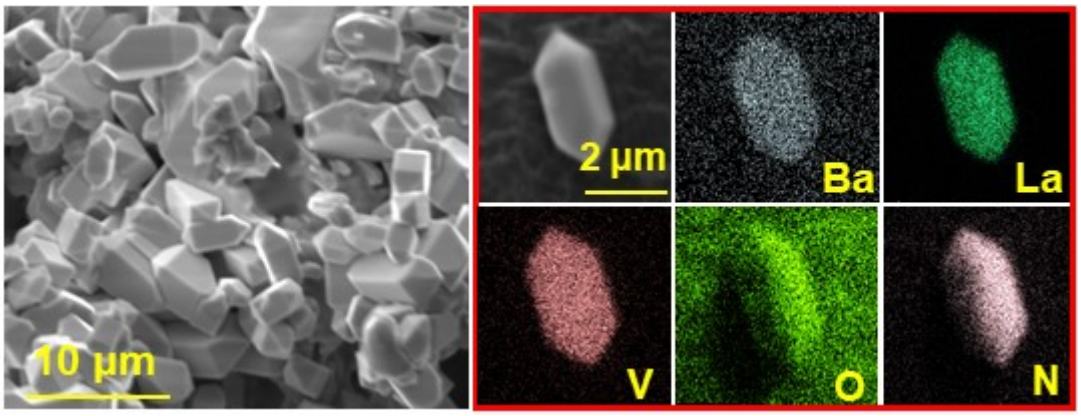

Figure S2. The SEM and EDX of $BaLa_5V_2O_3N_7$.

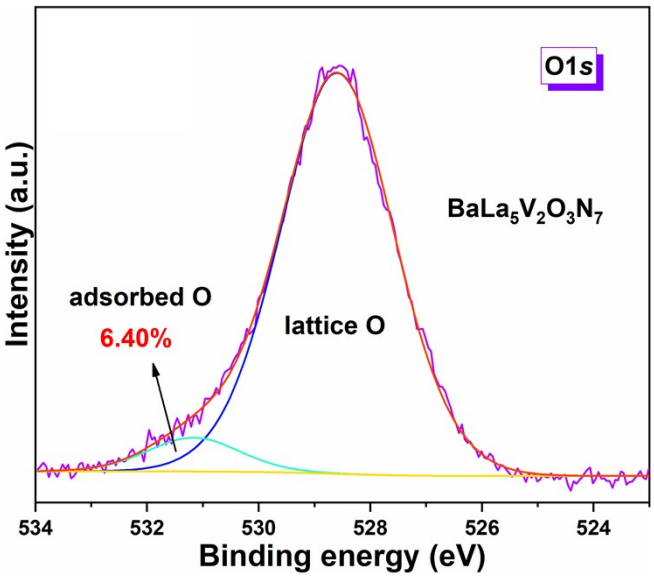

Figure S3. XPS spectra of O in $BaLa_5V_2O_3N_7$.

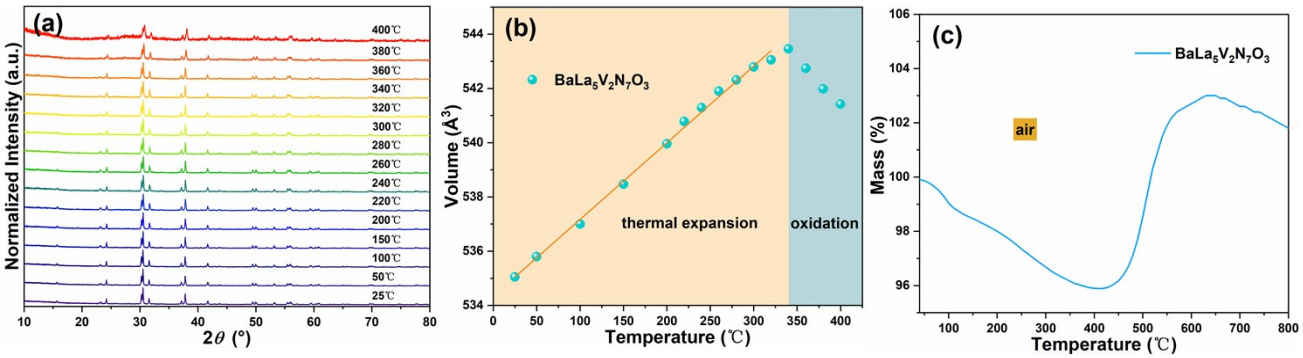

Figure S4. (a) VT-XRD pattern of $BaLa_5V_2O_3N_7$ sample; (b) Unit cell volumes (V) evolution of $BaLa_5V_2O_3N_7$ at different temperatures; (c) DSC curves of $BaLa_5V_2O_3N_7$.

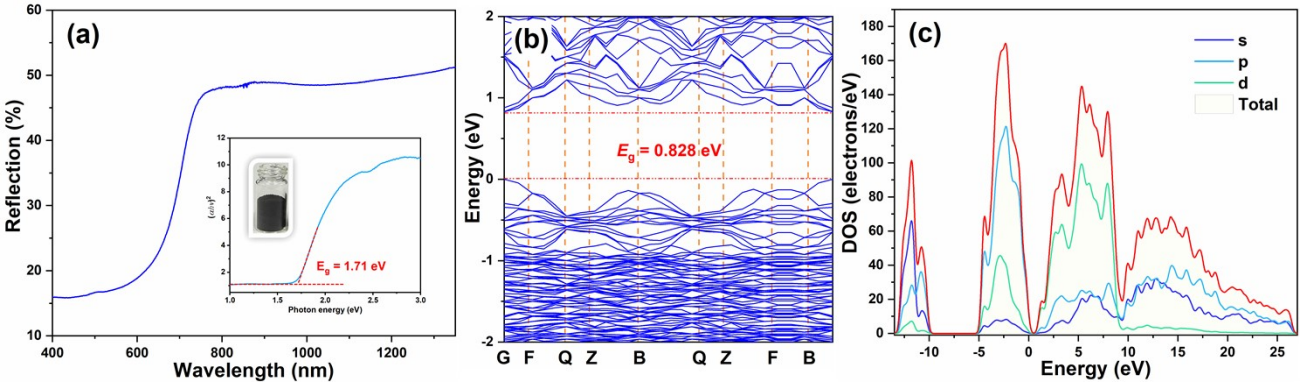

Figure S5. (a) UV-vision near-infrared diffuse reflection spectrum of $BaLa_5V_2O_3N_7$, the illustration shows the corresponding band gap calculation;(b) Electron band structure; (c) Total and orbital densities of states.

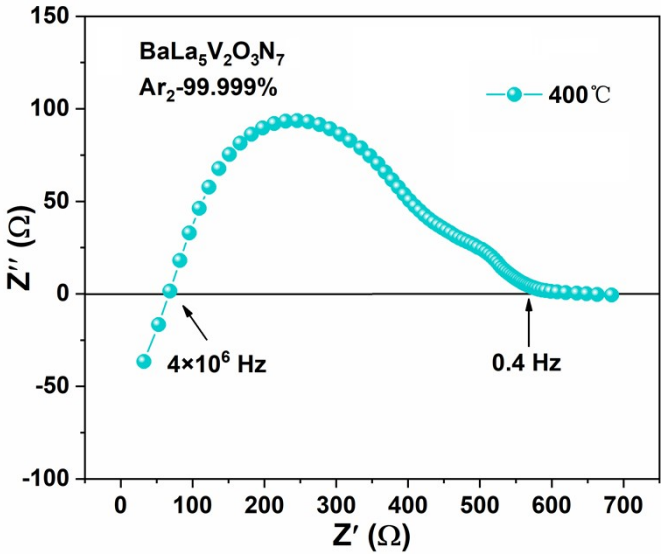

Figure S6. Complex impedance plot of $BaLa_5V_2O_3N_7$ at 400°C.

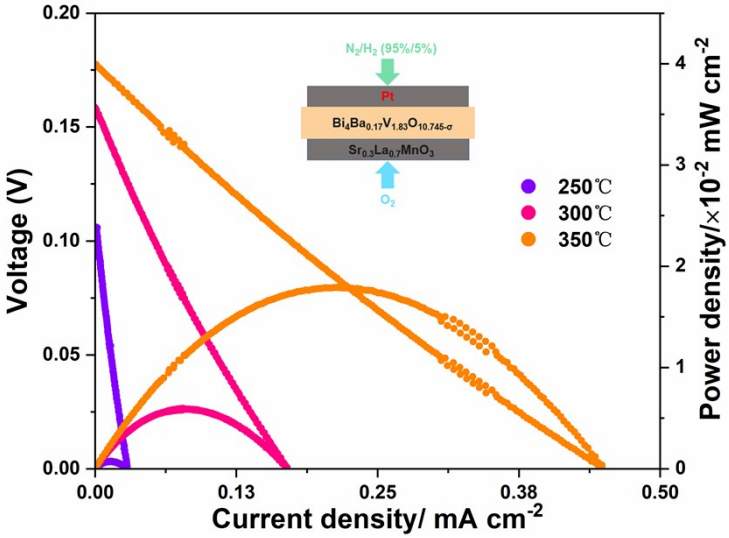

Figure S7. The I-V characteristics and power density curves of metal Pt as LT-SOFC anode at the temperature range of 250-350°C.

Reference

1 J. C. Li, L. Yang, J. G. Xu, A. J. Fernández-Carrión and X. J. Kuang, *Inorg. Chem.*, 2022, **61**, 5413-5424.

2 L. Gamperl, L. Neudert, P. Schultz, D. Durach, W. Schnick and O. Oeckler, *Combining Alkaline Earth and Rare Earth Metals in Oxonitrido (carbido) silicates as Luminescent Materials for Solid-State Lighting*, 2021, **27**, 87.

3 D. Durach, L. Neudert, P. J. Schmidt, O. Oeckler and W. Schnick, *Chem. Mater.*, 2015, **27**, 4832-4838.

4 B. Anke, T. Bredow, M. Pilarski, M. Wark and M. Lerch, *J. Solid State Chem.*, 2017, **246**, 75-80.

5 S. J. Clarke, P. R. Chalker, J. Holman, C. W. Michie, M. Puyet and M. J. Rosseinsky, *J. Am. Chem. Soc.*, 2002, **124**, 3337-3342.

6 J. Oró-Solé, L. Clark, W. Bonin, J. P. Attfield and A. Fuertes, *Chem. Commun.*, 2013, **49**, 2430-2432.
7 B. Almoussawi, *Material chemistry*. Université de Lille, 2021. English.
8 S. Nakhal, W. Hermes, T. Ressler, R. Pöttgen and M. Lerch, *Z. Anorg. Allg. Chem.*, 2009, **635**, 2016-2020.
9 C. Xia, Y. Q. Mi, B. Y. Wang, B. Lin, G. Chen and B. Zhu, *Nat. commun.*, 2019, **10**, 1707.